

## SECOND QUARTERLY REPORT

STUDIES OF REACTION GEOMETRY IN OXIDATION AND REDUCTION  
OF THE ALKALINE SILVER ELECTRODE

JPL 951554

This work was performed for the Jet Propulsion Laboratory,  
California Institute of Technology, sponsored by the National  
Aeronautics and Space Administration under Contract NAS7-100.

N 67 13213	(ACCESSION NUMBER)	(THRU)
28	(PAGES)	(CODE)
CR 80528	(NASA CR OR TMX OR AD NUMBER)	(CATEGORY)

FACILITY FORM 602

E. A. Butler  
A. U. Blackham  
Chemistry Department  
Brigham Young University  
Provo, Utah

October 10, 1966

GPO PRICE \$ \_\_\_\_\_  
CFSTI PRICE(S) \$ \_\_\_\_\_  
Hard copy (HC) 2.00  
Microfiche (MF) .50  
# 653 July 65

1 of 28

# ABSTRACT

13213

1. The measurement and recording of the difference in potential ( $\Delta E$ ) at two points on a working electrode with the simultaneous measurement of the electrode potential has been continued. These measurements have supplied data on relating the current distribution in an electrolytic cell to cell and electrode geometry and electrolyte concentration. Simultaneous plots of the  $\Delta E$  curve, the potential-time curve, and the differential of the potential-time curve are presented.
2. Silver surfaces have been prepared on glass by evaporation-deposition, and used as standard electrodes in surface area determinations of various silver surfaces. A standard curve used as a base for surface area determinations has also been obtained. Surface areas of from 2 to 4 cm<sup>2</sup> have been estimated by the technique to within  $\pm 5\%$ .
3. Our observations indicate the presence of an organic residue on commercial sintered silver electrode part of which is hydrocarbon in character and part of which is carbonaceous. The weight per cent of this residue is 0.01 - 0.03%. Carbon dioxide is observed as the major product of the pyrolysis in oxygen.

## I. Potential Variations Over the Electrode Surface.

### Apparatus and Reagents

The test electrodes were constructed from silver foil, 0.011 cm thick, which was 99.99% pure. Square electrodes 2 cm on a side and round electrodes 1.80 cm in diameter were prepared from the foil. The electrodes were cleaned with cleansing powder, (Comet brand) and rinsed in distilled water before use. Other cleaning methods were tried, but no difference in the results was noted. The counter electrode used in all experiments with a suspended test electrode was a 2 x 2 cm platinum foil. For those experiments using a point source counter electrode, a 1.80 mm platinum sphere was made by melting the end of a platinum wire which was sealed in the end of a glass rod.

Solutions of 0.1 N and 1 N KOH were prepared from reagent grade KOH. All other KOH solutions were made by diluting the 0.1 N solution. The ammoniacal electrolyte was 14.8 N in  $\text{NH}_4\text{OH}$  and 0.1 N in  $\text{KHO}_3$ . The potassium nitrate was added to increase the conductivity of the solution.

The test cell and Luggin capillary measuring circuit were the same as described in the First Quarterly Report (July 9, 1966) page 1 and Figure 1. All experiments using electrodes suspended in the electrolyte were performed in this cell. A rectangular trough (4.5 x 4.5 x 25.4 cm) with the silver foil test electrode covering completely one end and the platinum foil counter electrode covering the other end, similar in design to a Haring<sup>1</sup> cell, except for the two gauze electrodes, was also constructed.

### Experiments and Results

#### 1. Electrolyte Concentration Experiments

Edge to center potential differences on the surface of a square suspended silver electrode during oxidation and reduction at 1.30 ma/cm<sup>2</sup>

in solutions of  $1N$ ,  $0.11N$ ,  $0.055N$ ,  $0.028N$ , and  $0.014N$  KOH were recorded. The  $\Delta E$  values of the peaks, which correspond with reaction changes, are recorded in Table 1. The  $\Delta E$ 's are seen to be inversely related to KOH concentration. The oxidation time was much longer for the highest concentration.

## 2. Potential Mapping Experiments

A series of  $\Delta E$  measurements was made around a suspended circular silver electrode in the ammoniacal and the  $0.1 N$  KOH electrolytes. Ammonia prevents, by the formation of silver ammine complexes, the build-up of  $Ag_2O$  on the electrode and the reaction change which follows that build-up. Results obtained in both solutions were similar, but plotting was simplified when no reaction change occurred. From the measurements made in the ammoniacal solution, equipotential lines (40 mv apart) were constructed. (Figure 1.) Plots of the potential difference from the center of the electrode to points along its radius at various distances from the electrode are shown in Figure 2. All measurements were made with one capillary fixed in the center which was arbitrarily given the value of zero.

## 3. Haring Cell Experiments

A Haring cell was used for potential difference measurements since it is thought to give a uniform current distribution (Haring<sup>1</sup>, Kasper<sup>2</sup>). Measurements were made on various areas of the Ag electrode and the Pt electrode with the ammoniacal and the  $0.1 N$  KOH electrolytes.  $\Delta E$  values were also measured on the Ag electrode using a platinum sphere counter electrode placed at various distances from the silver.

No  $\Delta E$  was measured from center to edge at the silver electrode when the cell was filled with ammonia. With KOH no significant  $\Delta E$ 's were measured on the platinum electrode. These results help substantiate the assertion that current distribution is uniform in the Haring cell. Yet  $\Delta E$  measurements from the edge to center

of the silver electrode in KOH still showed two large peaks during oxidation and two more during reduction. These peaks always occurred at the time of a reaction change on the silver electrode i. e. the change from  $\text{Ag} = \text{Ag}_2\text{O}$  to  $\text{Ag}_2\text{O} = \text{AgO}$  (Figure 4 Curve D).

For other experiments a 1.8 mm platinum sphere was substituted for the foil counter electrode in the Haring cell. The edge to center  $\Delta E$  values measured with the platinum sphere counter electrode at various perpendicular distances from the silver electrode are recorded in Table 2. At distances farther back than 2 cm the potential at the edge was more anodic and at distances closer than 2 cm the potential at the center was more anodic (during oxidation) than the potential at the edge. At distances within 2 cm of the silver electrode and with high current densities a reaction such as the formation of AgO or the evolution of oxygen was observed to begin at the center and then spread out to the edges of the electrode. The extremely non-uniform current distribution obtained by placing the platinum sphere very close to the 4.5 x 4.5 cm silver foil electrode helps account for these observations.

#### 4. Simultaneous $\Delta E$ , Potential, and Potential Differential Experiments

Simultaneous  $\Delta E$ , potential, and potential-differential curves were made using a third mercury-mercuric oxide reference electrode. The differential of the potential-time curve was obtained with an operational amplifier differentiator. (Figure 3). The simultaneous curves (Figure 4) show that  $\Delta E$  peaks correspond with changes in the reaction potential.

### Discussion

It is probable that the potential differences ( $\Delta E$ ) which we have measured in the test cells arise from at least two different phenomena. The first and most widely considered in the literature<sup>2, 3, 4</sup>, is an unequal current distribution caused by the geometry of the electrodes

and the cell. The second is an unequal oxidation of the electrode where one portion of the electrode is farther along the potential-time curve than another (see First Quarterly Report page 3), and seems to be of significant effect only at the time of a reaction change on the silver electrode (i. e. the change from  $\text{Ag} = \text{Ag}_2\text{O}$  to  $\text{Ag}_2\text{O} = \text{AgO}$ ).

The first phenomenon could best be investigated in an electrolyte where there is no change in reaction and thus no change in electrode potential. This is the case when a silver electrode is oxidized in an ammoniacal electrolyte. An extension of arguments, made by Wagner<sup>3</sup> about current distribution in the electrolytic cell would explain the shape of the equipotential lines (Figure 1) found for the suspended silver electrode in the ammoniacal electrolyte. Similar arguments by others<sup>1, 2</sup> also predict that no potential differences should exist on the silver anode in the Haring cell filled with the ammoniacal electrolyte, because of the uniform current distribution in that cell.

Several authors<sup>4, 5</sup> have shown that if a counter electrode is used which is small in size compared to the working electrode the current density between them will be greatest in the region near the small electrode. This was the result obtained with the 1.8 mm platinum sphere counter electrode placed at distances less than 2 cm from the working electrode in the 0.1 N KOH electrolyte. At high current densities (10 ma/cm<sup>2</sup>) it was also possible to see a reaction such as the evolution of oxygen begin first in the area near the platinum, sphere and then expand radially over the remainder of the electrode. An attempt was made to measure the  $\Delta E$  between the center and edge under these conditions where there was visible evidence for large potential differences. The largest  $\Delta E$  of 400 mv was measured during the reduction reaction where free silver was seen in the center portion of the electrode under one measuring capillary while the yet unreduced silver oxide was seen covering the edge area

under the second measuring capillary. The  $\Delta E$  curve rose to the 400 mv peak as the border between the free silver and the silver oxide moved out in a circle of increasing radius and attained its highest value just before the border crossed beneath the second capillary tip.

The Haring cell with the ammoniacal electrolyte is a system which has a uniform current density, and thus no potential difference was measurable. When this cell was altered by using a small platinum sphere instead of platinum foil as counter electrode the results show a higher current density near the sphere. A non-uniform current distribution was also found around a suspended electrode in the ammoniacal electrolyte. All of these results are in agreement with existing literature and can be predicted by arguments based on the geometry of the electrodes and the cell.

The second phenomenon is apparently not caused by large inequalities in the current distribution, for large peaks occurred (Figure 4 curve D) in the  $\Delta E$  curve in the Haring cell using the 0.1 N KOH electrolyte. These peaks were associated with changes in the cell reaction and thus correspond to the steep portions of the potential-time curve. In each case the edge was found to be more anodic than the remainder of the electrode during oxidation of the silver.

Examination of the  $\Delta E$  curves of the suspended electrode suggests that these curves may be a combination of both unequal current distribution and unequal oxidation. Addition of curves D and E to form curve C in Figure 5 illustrates this.

Table 3 shows a reversal in the  $\Delta E$  from more anodic at the center to more anodic at the edge as the platinum sphere counter electrode is moved away from the 4.5 x 4.5 cm silver foil electrode which was sealed in the end of the Haring cell (0.1 N KOH electrolyte). This may also be the combination of the two phenomena mentioned, the second masking the first as the counter electrode is moved farther than 2 cm

from the working electrode.

The results recorded in Table 1 show the inverse relationship of the  $\Delta E$  to electrolyte concentration. Preliminary experiments indicate that these  $\Delta E$  changes are not entirely dependent on conductivity changes which accompany electrolyte concentration changes. This suggests that a kinetic effect dependent on hydroxide ion concentration may be in part responsible for the changes in the measured  $\Delta E$ .



### Proposals for Further Work

We plan to do the following experiments:

1. We plan to establish equipotential maps such as we have in Figure 1 for several different electrode and cell configurations.
2. We will use the ammoniacal electrolyte for a series of runs at different temperatures to determine how temperature and the accompanying conductivity changes affect the  $\Delta E$ .
3. We will investigate a variety of electrolytes and electrolyte concentrations and their effects on the  $\Delta E$ .
4. We propose experiments to determine the effect of stirring on the  $\Delta E$  at low ( $\ll 0.1$  N KOH) electrolyte concentrations.

## II. Surface Area Estimation

### Depth of Oxidation

When the potential of a silver electrode is recorded during a constant current oxidation in alkaline solution, the curve recorded has a plateau denoting a constant potential during the formation of the layer of silver (I) oxide. The length of this plateau represents the time in minutes,  $t$ , during which this reaction occurs. The thickness of the surface layer of the silver through which this reaction occurs is called the depth of penetration,  $x$ , and is given by the equation

$$X = \frac{No}{F \left[ \rho \frac{No}{M} \right]^{2/3}} \cdot \frac{It}{a} = kDt$$

where

- $x$  = number of monolayers of penetration
- $No$  = Avogadro's number
- $F$  = Faraday
- $\rho$  = density in g. / cm<sup>3</sup> -
- $M$  = atomic weight (g. /mole)
- $I$  = current (amps.)
- $a$  = surface area (cm<sup>2</sup>)
- $t$  = plateau length (minutes)
- $D$  = current density (amps. /cm<sup>2</sup>)
- $k$  = a constant

If the assumption is made that at a given current density, the depth of penetration, on the average, will be equal for smooth as well as uneven surfaces, the following result is obtained:

Assume that if  $D_1 = D_2$  then  $X_1 = X_2$ .

Therefore  $X_1 = K D_1 t_1 = K D_2 t_2 = X_2$  and  $t_1 = t_2$

This means that if two electrodes have equal plateau lengths, they were oxidized at the same current density and have equal depths of penetration.

A standard curve of known current density versus plateau length, expressed in minutes, has been plotted. (See Figure 6) From this curve, unknown surface areas have been determined. By changing the applied current until the plateau length matches a point on this standard curve a cross reference to the known current density can be obtained, and thus the unknown surface area may be determined.

Glass discs of 18 mm diameter ( $2.54 \text{ cm}^2$  surface area) which have had a silver film deposited upon them by vacuum vaporization have been used as the standard electrodes.<sup>7</sup> The main problem experienced with these electrodes has been the poor adhesion of the silver to the glass.<sup>8</sup> Without proper adhesion, the silver tends to dissolve off the discs during the oxidation run. This problem has been overcome by first cleaning the discs in soap and water and then in alcoholic potassium hydroxide solution. They are then rinsed in distilled water and wiped dry with lint-free tissue. The rubbing of the glass puts a static charge on the surface of the discs which appears to help the adhesion of the silver to the glass. Using these discs we have been able to reproduce oxidation runs to within 3 to 7 per cent. (See Table 3)

These silver discs were oxidized as described in the First Quarterly Report using the same reagents and circuitry. Because of the temperature dependence of the depth of oxidation the reaction cell has been thermostatted to  $27.5 \pm .5^\circ \text{C}$ .<sup>6</sup>

X-ray studies of silver films produced by vacuum deposition indicate that the gross crystal structure produced is almost identical to that observed in sintered silver plates. Furthermore, the thicker the film deposited the more nearly the surface area of the film approaches the surface area of the glass substrate<sup>9</sup>. The films used in these experiments are on the order of 3000 to 4000 monolayers thick, and therefore their surface areas should approach the geometrical areas of the glass discs to well within our experimental limits.

In order to check the standard curve, a larger electrode of known

surface area was used. To do this 22 mm diameter glass discs ( $3.80 \text{ cm}^2$  surface area) were prepared in the same manner as the standard electrodes. These discs were then oxidized and the plateau length matched with the standard curve. The experimental surface area agreed to within 1 per cent in the regions of greatest change of the curve (Figure 6) and to within 9 per cent in the flatter regions of the curve.

One might expect a difference in the depth of oxidation in ordinary rolled silver foil as compared with these vapor deposited films because of a difference in the number of lattice imperfections per unit volume. The experimental evidence, however, indicates that the depth of oxidation is the same in rolled silver foil as in the vapor deposited silver. The reason for this conclusion is our observation that the roughness factor for the rolled silver foil is 1.3 and this is the same value for nickel foil obtained by double-layer capacitance measurements.<sup>10</sup> Therefore, the standard curve should be useful for surface area determinations of rolled silver foil of low roughness factors and for sintered silver electrodes of high roughness factors. (Table 4)

#### Proposal for Further Work

We will increase the surface area of silver foil electrodes by carefully controlled means until larger surface areas of the order of those of sintered silver plates can be determined with confidence.

### III. Organic Residues in Sintered Silver Electrodes

Determinations of the products from pyrolysis of sintered silver electrodes were reported in the First Quarterly Report of this contract, JPL 951554. These products were water, ethylene, methane, nitrogen, and oxygen of which the ethylene and methane were confirmed by infrared spectrophotometry. Carbon dioxide and ethane were indicated in the gas chromatographic analyses but had not been confirmed. We now report that sufficient carbon dioxide has been obtained in some analyses to confirm the assignment of carbon dioxide. The component in the gas chromatographic analyses having the retention time of a standard sample of carbon dioxide was shown to have the characteristic infrared absorption at  $2350\text{ cm}^{-1}$ .

A new borosilicate glass pyrolysis chamber was constructed. A schematic diagram of this chamber is shown in Figure 7. This chamber, as compared with the one previously used, permits more convenient change of samples and eliminates the problem of the carrier gas leaking at the joints.

Several samples have been pyrolyzed with oxygen as the carrier gas. The following table shows a comparison of the carbon dioxide and water observed with helium and oxygen as carrier gases.

Experiment	Amount of Silver (moles)	Analysis	
		Carbon Dioxide (moles)	Water (moles)
1. Sintered silver pyrolyzed at $500^{\circ}\text{C}$ in helium	$1.0 \times 10^{-2}$	$1.5 \times 10^{-6}$	$4.9 \times 10^{-6}$
2. Sintered silver pyrolyzed at $500^{\circ}\text{C}$ in oxygen	$1.0 \times 10^{-2}$	$9.1 \times 10^{-6}$	$5.5 \times 10^{-6}$

The carbon dioxide increases when the sample is pyrolyzed in oxygen. This suggests reaction of the oxygen with a carbonaceous residue. If the residue had more of a saturated hydrocarbon character a parallel increase in the amount of water would be expected when the sample was pyrolyzed in oxygen. However, the water remained the same.

In the catalytic oxidation of ethylene by silver with limited oxygen, Twigg<sup>(11)</sup> has observed the formation of a non-volatile deposit on the surface of the silver catalyst. This deposit may be comparable to the deposit observed in this work.

Four samples of commercial sintered silver electrodes are compared in Tables 5 and 6. The quantitative results are about the same for these samples with the exception that the Yardney electrode gave about twice the carbon dioxide that the others gave. These results indicate that there is approximately 0.1 to 0.3 milligram of carbon and 0.01 to 0.02 milligram of hydrogen per gram of sintered silver electrode. The question of whether or not some of the hydrogen is present as strongly absorbed water has not been resolved yet.

The pyrolyses in helium of three samples of commercial sintered silver are compared in Table 7. The light gases are not resolved with the silica gel column. Carbon dioxide is the major component with smaller amounts of ethylene and ethane. The carbon dioxide in part may come from the oxidation of some of the carbonaceous deposit by the small amount of oxygen present as an impurity in the carrier gas.

Runs have been made in which samples of the Delco-Remy electrode were pyrolyzed at 650°C in hydrogen. The products were analyzed with the silica gel column. The results show that for a 1.0 gram sample of silver electrode the following products are obtained:

methane	0.025 mg.
carbon monoxide	0.013 mg.
ethane	0.009 mg.
carbon dioxide	0.0009 mg.

Pyrolysis in hydrogen appears to convert carbon dioxide to carbon monoxide, possibly by catalytic action of the stainless steel tube in which this pyrolysis was made. Also it is observed that pyrolysis in hydrogen gives ethane and no ethylene where pyrolysis in helium usually gives more ethylene than ethane.

The model that accounts for our observations at this stage of investigation is a sintered silver electrode containing a small amount of an organic residue part of which is sufficiently characteristic of saturated hydrocarbons to give methane and ethylene on pyrolysis and part of which is more carbonaceous in nature which remains on the silver during pyrolysis in helium but which forms carbon dioxide when pyrolyzed in oxygen. Approximately 80-90% of the residue is of this latter type.

#### Proposal for Further Study

Some runs will be made with high purity helium as carrier gas to minimize any oxidation due to oxygen as impurity in the carrier gas.

Further effort will be made to determine amounts of methane and carbon monoxide with hydrogen as the carrier gas.

Table 1  
The Effect of Electrolyte Concentration  
on Edge to Center  $\Delta E$  Measurements

Normality of KOH	Specific Conductivity (ohm <sup>-1</sup> cm <sup>-1</sup> ) (measured)	Oxidation Time (min.)	$\Delta E$ Peaks *				
			#1(mv)	#2(mv)	#3(mv)	#4(mv)	#5(mv)
1.0	20.1 x 10 <sup>-2</sup>	14.0	1.0	1.5	3.0	1.5	2.5
1.0		13.3	1.3	1.2	3.5	1.7	2.2
0.11	2.66 x 10 <sup>-2</sup>	1.6		7.8	18.5	14.5	16.0
0.11		1.8		8.0	14.5		24.5
0.055	1.34 x 10 <sup>-2</sup>	1.3	10.5	17.5	15.0		20.5
0.028	0.68 x 10 <sup>-2</sup>	0.8		17.0	35.0	6.5	35.5
0.014	0.34 x 10 <sup>-2</sup>	1.3		24.0	>45	29.0	>55

\* The peaks #1 to #5 are those labeled on the  $\Delta E$  curve C in Figure 4. The same silver foil electrode was cleaned before each run by the method described on page 1 of this report.

Table 2  
 $\Delta E$  Measurements in the modified Haring cell  
using a point source counter electrode

Distance from Ag electrode	$\Delta E$ Peaks *			
	#1 (mv)	#2 (mv)	#3 (mv)	#4 (mv)
1.0 cm	-16	-45	9	32
1.3 cm				18
2.0 cm	4	8		
2.0 cm	5	14	0	-6
2.3 cm	1	12		-18
2.8 cm	9	29	-11	-30
2.8 cm	11	27	-10	-26
5.0 cm	10	38	-14	-60
5.0 cm		>30	-6	<-30
7.5 cm	18	44	-8	-54

\* The peaks #1 to #4 are those labeled on the  $\Delta E$  curve D in Figure 4



TABLE 3

## Reproducibility of Oxidation Runs

Current Density ( $\mu$ amp/cm <sup>2</sup> )	Plateau Length (minutes)		Deviation
80.8	21.6	$\pm$	3.5%
97.9	15.4	$\pm$	2.9%
101	11.7	$\pm$	3.2%
158	8.3	$\pm$	2.4%
236	4.6	$\pm$	4.3%
355	2.6	$\pm$	2.9%
693	.75	$\pm$	6.6%

TABLE 4

## Surface Area Estimation

Type of Surface	Surface Area		Roughness Factor
	Geometrical	Experimental	
Silver deposited upon glass disc (22mm) at three current densities	3.80 3.80 3.80	3.76 3.82 3.46	0* 0 0
Unpolished silver foil, cleaned with soap and water, same current density	2.54 2.54	3.30 2.79	1.3 1.1
Silver wire cleaned with soap and water, same current density	5.00 5.00 5.00	5.14 5.23 5.02	1.03 1.05 1.01

\*By theory silver on glass should be a smooth surface. Errors are due to graph or inaccuracy.

Nickel foil by double layer capacitance

1.3

TABLE 5

Gas Chromatographic Analysis of Products from Pyrolysis of Sintered  
Silver Electrodes in Oxygen

Conditions: Temperature of Pyrolysis 500°C  
n-Decyl Phthalate Column, 3 feet  
Temperature of Column 100°C  
Carrier Gas, Oxygen at 15 psi

Sample	Analytical Data					
Designation	Weight Grams	Specific Retention Peak	Retention Time(min)	Relative Peak Area	Assignment	Weight Milligrams
1. Delco-Remy #1	1.164	1	1.2	1.34	CO <sub>2</sub>	0.40±.06 *
		2	6.8	1.31	H <sub>2</sub> O	0.10±.01
2. Delco-Remy #2	.945	1	1.2	1.72	CO <sub>2</sub>	0.47
		2	7.2	1.23	H <sub>2</sub> O	0.10
3. Electric Storage Battery	1.160	1	1.2	1.67	CO <sub>2</sub>	0.40
		2	6.7	1.59	H <sub>2</sub> O	0.14
4. Yardney	1.072	1	1.2	2.11	CO <sub>2</sub>	0.56
		2	6.4	1.75	H <sub>2</sub> O	0.16
<u>Standards</u>						
CuSO <sub>4</sub> ·5H <sub>2</sub> O	.0005	1	6.2	2.65	H <sub>2</sub> O	.18
CO <sub>2</sub>	.53	1	1.6	1.92	CO <sub>2</sub>	.53

\*limits based of 4 determinations

Table 6

Gas Chromatographic Analysis of Products from  
Pyrolysis of Sintered Silver Electrodes in Oxygen

Conditions: Temperature of Pyrolysis, 500°C;  
Silica Gel Column, 4 ft;  
Temperature of Column, 29°C;  
Carrier Gas, Oxygen at 15 psi.

Samples		Analytical Data				
Designation	Weight grams	Specific Peak	Retention Time (min)	Relative Peak Area	Assignment	Weight milligrams
1. Delco-Remy #1	1.153	1	.7	.07	CO <sub>2</sub>	0.51
		2	1.1	.07		
		3	7.2	1.52		
2. Electric Storage Battery	1.069	1	.7	.02	CO <sub>2</sub>	0.52
		2	1.1	.02		
		3	7.2	1.69		
3. Delco-Remy #2	1.251	1	.7	.02	CO <sub>2</sub>	0.52
		2	1.1	.02		
		3	7.2	1.69		
4. Yardney	.903	1	.7	.04	CO <sub>2</sub>	0.87
		2	1.1	.08		
		3	7.2	3.06		
<u>Standard</u>						
CO <sub>2</sub>	.75	1	6.7	2.65	CO <sub>2</sub>	0.75

Table 7

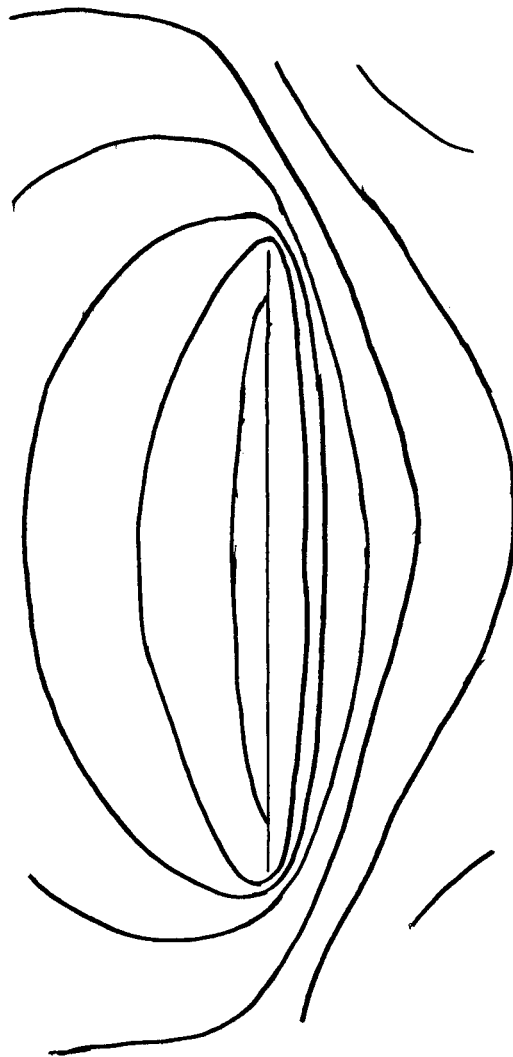
Gas Chromatographic Analysis of Products from  
Pyrolysis of Sintered Silver Electrodes  
in Helium at High Temperatures

Conditions: Silica Gel Column, 4 feet;  
Column Temperature, 30°C;  
Carrier Gas, Helium at 15 psi.

Designation	Samples Weight grams	Temp. of Pyrolysis °C	Light Gases O <sub>2</sub> , N <sub>2</sub> , CH <sub>4</sub> , CO	Analytical Data (milligrams)		
				C <sub>2</sub> H <sub>6</sub>	CO <sub>2</sub>	C <sub>2</sub> H <sub>4</sub>
1. Electric Storage Battery	1.424	750*	0.060 mg	0.00057 mg	0.11 mg	0.0030 mg
2. Delco-Remy	1.039	750	0.160	0.0022	0.13	0.00085
3. Yardney	0.944	500	0.012	0.0023	0.035	0.0045

Figure 1

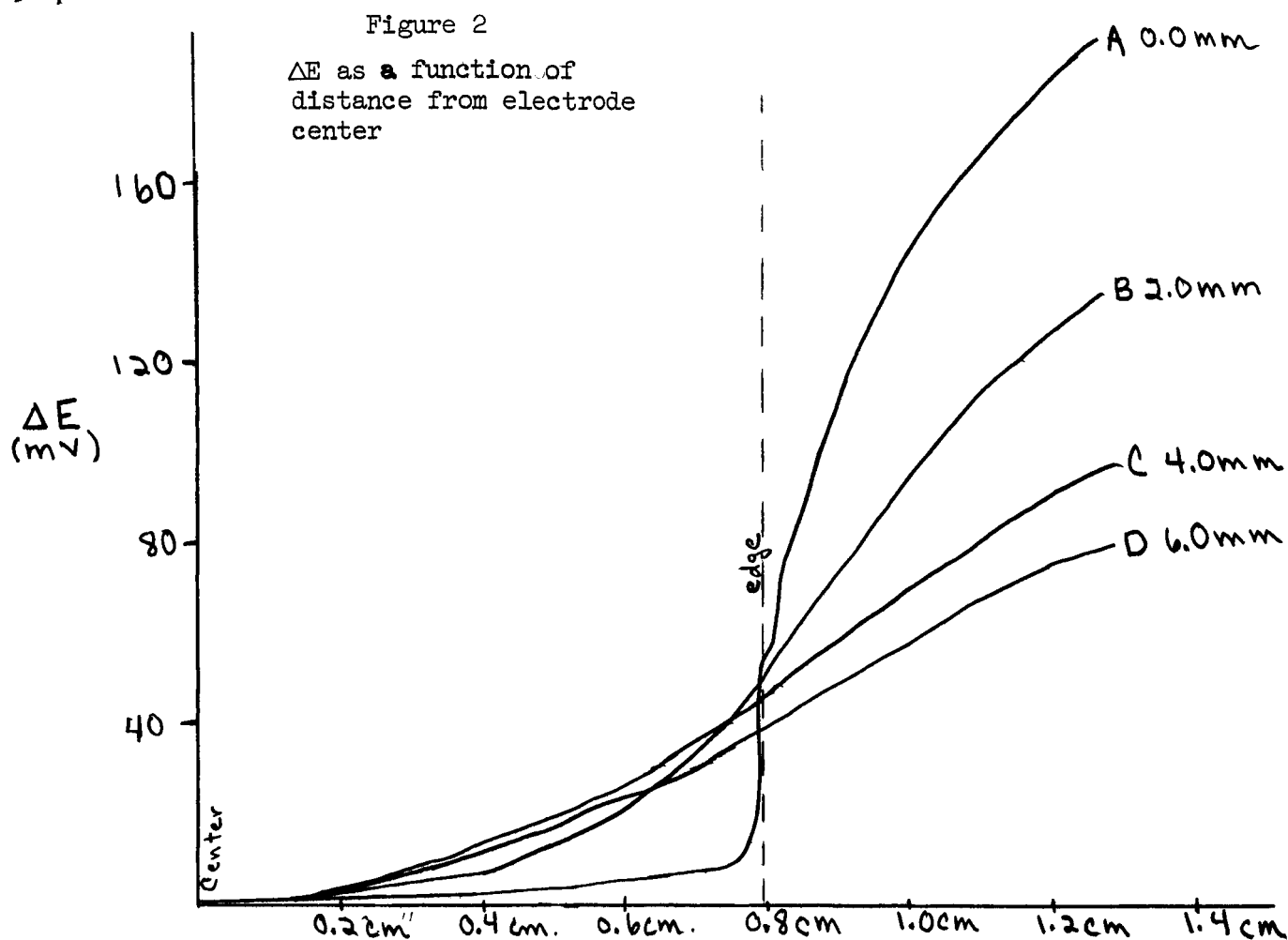
Equipotential map of working suspended silver electrode



To counter electrode  
↓

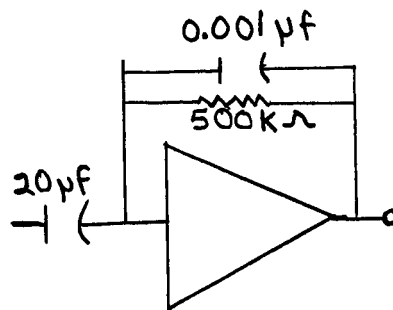
(The equipotentials are on a plane normal to electrode surface cutting the electrode at its diameter and are 40 mv apart.)

[scale 1cm = 0.1cm] 20



- A. Measurements were made in the plane of the electrode surface.  
 B. Measurements were made 2.0 mm away from the plane of the electrode surface.  
 C. 4.0 mm away... D. 6.0 mm away.....

All measurements were made in reference to one capillary which was fixed at the center of the electrode surface and were normalized to  $\Delta E = 0$  when the second capillary was at the center or any position (2.0, 4.0, and 6.0 mm) normal to the center.



Operational Amplifier as differentiator

Figure 3

$$\begin{array}{c} \text{Ag} = \text{Ag}_2\text{O} \\ \text{Ag}_2\text{O} = \text{AgO} \\ \text{OH}^- = \text{O} \\ \text{AgO} = \text{Ag}_2\text{O} \\ \text{Ag}_2\text{O} = \text{Ag} \end{array}$$

2

3

$H_2O =$

E

E Curve of the Haring cell electrode in 0.1N KOH

1 2 3 4 5

Oxidation Reduction

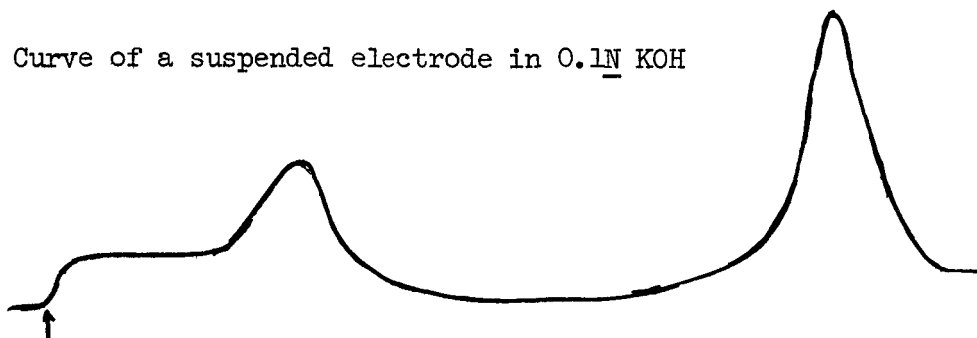
## Simultaneous Runs

Curves A, B and C were made at the same time. Curve D was made separately with a simultaneous potential-time curve and then matched to curve A of this figure.

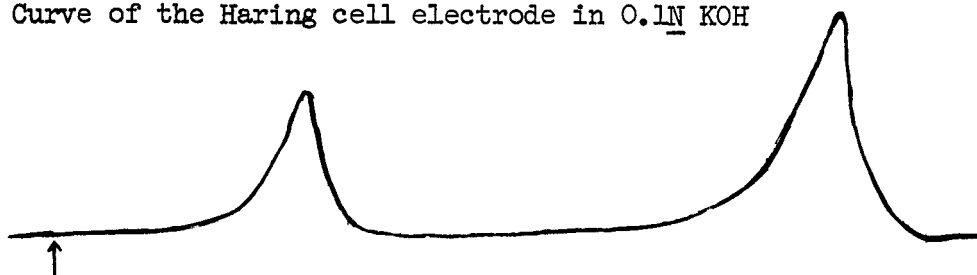


Comparison of three  $\Delta E$  curves made during the oxidation of silver electrodes. (curves C and D also appear in Figure 4)

C.  $\Delta E$  Curve of a suspended electrode in 0.1N KOH

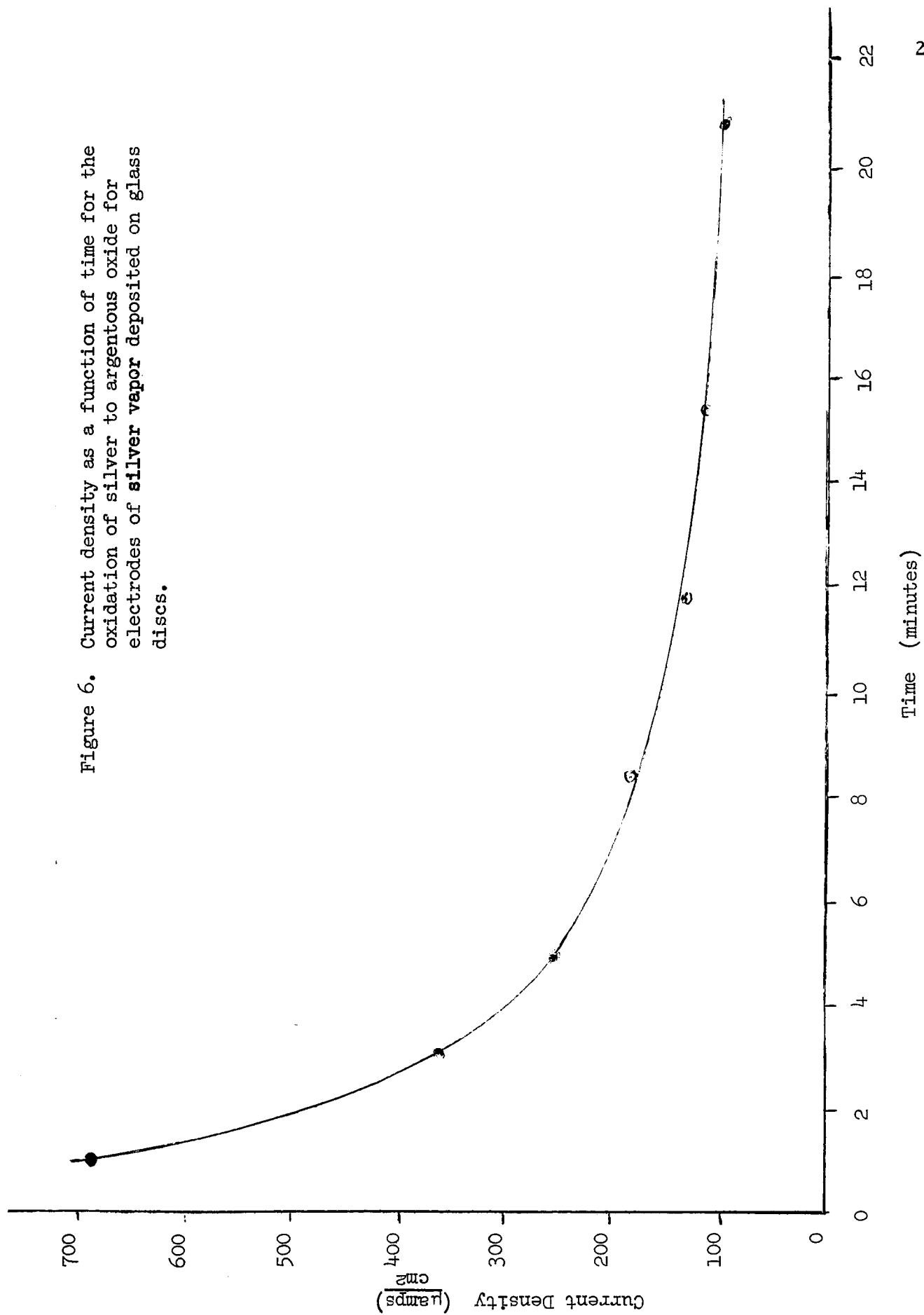


D.  $\Delta E$  Curve of the Haring cell electrode in 0.1N KOH



E.  $\Delta E$  Curve of a suspended electrode in the ammoniacal electrolyte





1. Incoming stream of carrier gas
2. O-ring assembly (clamp not shown)
3. 3-way stop-cock
4. Outgoing carrier gas
5. Position of sample
6. Pyrolysis chamber

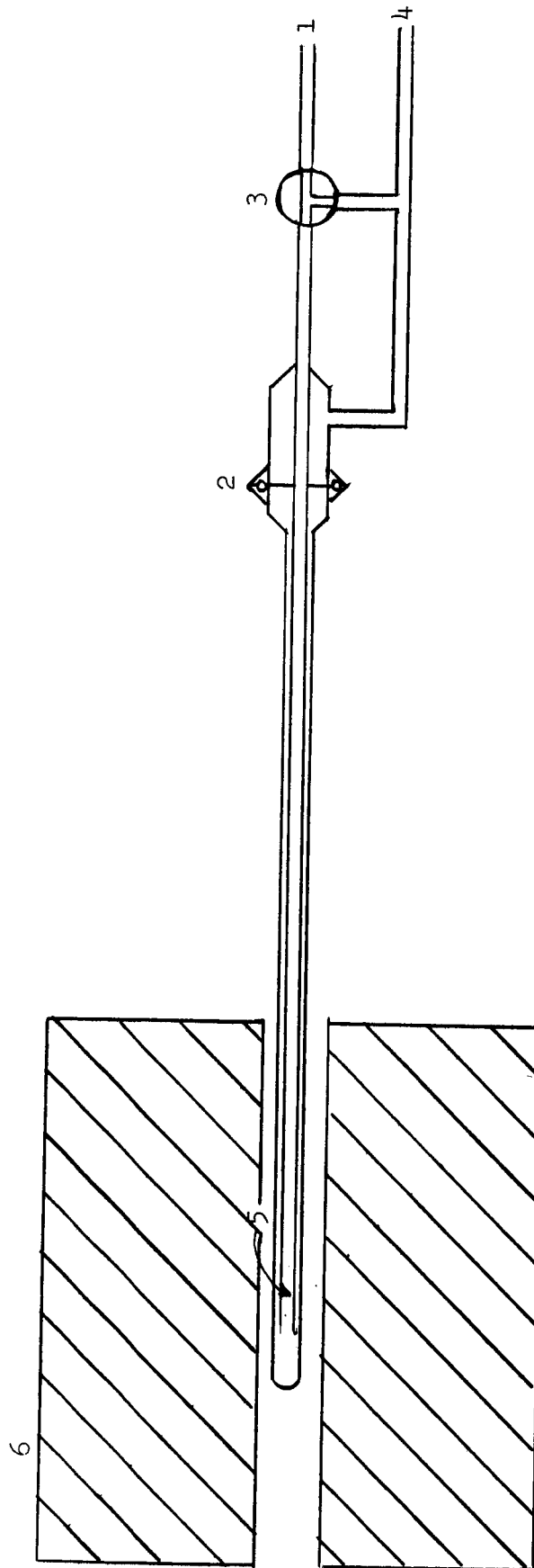


Figure 7. Pyrolysis Chamber

## REFERENCES

1. H. E. Haring, Trans. Electrochem. Soc., 49, 417 (1926).
2. C. Kasper, Trans. Electrochem. Soc., 77, 353 (1940).
3. C. Wagner, J. Electrochem. Soc., 98, 116 (1951).
4. I. Shain, Anal. Chem., 38, 1148 (1966).
5. G. L. Booman, W. B. Holbrook, Anal. Chem. 35, 1793 (1963).
6. J. A. Allen, Trans. Faraday Soc., 48, 273 (1952).
7. L. O. Olsen, C. S. Smith, E. C. Crittenden, Jr., J. App. Phys., 16, 425-33 (1945).
8. Allpress, Sanders, J. Catalysis, 3, 528-38 (1964).
9. R. L. Mass, Trans Faraday Soc., 59, 216-29 (1963).
10. J. McCallum, J. E. Walling, and C. C. Faust, "Measurement of True Surface Area in Electrode," First Quarterly Technical Progress Report, Battelle Memorial Institute, Columbus, Ohio (undated).
11. G. H. Twigg, Proc. Roy. Soc. London, A188 92-104 (1946).